eLife

Reviewed Preprint
v2 • October 16, 2024
Revised by authors

Reviewed Preprint
v1 • December 11, 2023

Neuroscience

HI-FISH: Whole brain in situ mapping of neuronal activation in *Drosophila* during social behaviors and optogenetic stimulation

Kiichi Watanabe, Hui Chiu, David J Anderson

Division of Biology and Biological Engineering, Tianqiao and Chrissy Chen Institute for Neuroscience, California Institute of Technology, Pasadena, CA USA • International Center for Cell and Gene Therapy, Fujita Health University, Toyoake, Japan • Department of Medical Research for Intractable Disease, Fujita Health University, Toyoake, Japan • Department of Immunobiology, Yale University School of Medicine, New Haven, CT USA • Howard Hughes Medical Institute, USA

Abstract

Monitoring neuronal activity at single-cell resolution in freely moving *Drosophila* engaged in social behaviors is challenging because of their small size and lack of transparency. Extant methods, such as Flyception, are highly invasive. Whole-brain calcium imaging in head-fixed, walking flies is feasible but the animals cannot perform the consummatory phases of social behaviors like aggression or mating under these conditions. This has left open the fundamental question of whether neurons identified as functionally important for such behaviors using loss- or gain-of-function screens are actually active during the natural performance of such behaviors, and if so during which phase(s). Here we perform brain-wide mapping of active cells expressing the Immediate Early Gene *hr38* using a high-sensitivity/low background FISH amplification method called HCR-3.0. Using double-labeling for hr38 mRNA and for GFP, we describe the activity of several classes of aggression-promoting neurons during courtship and aggression, including P1^{a} cells, an intensively studied population of male-specific interneurons. Using HI-FISH in combination with optogenetic activation of aggression-promoting neurons (opto-HI-FISH) we identify candidate downstream functional targets of these cells in a brain-wide, unbiased manner. Finally we compare the activity of P1^{a} neurons during sequential performance of courtship and aggression, using intronic vs. exonic *hr38* probes to differentiate newly synthesized nuclear transcripts from cytoplasmic transcripts synthesized at an earlier time. These data provide evidence suggesting that different subsets of P1^{a} neurons may be active during courtship vs. aggression. HI-FISH and associated methods may help to fill an important lacuna in the armamentarium of tools for neural circuit analysis in *Drosophila*.

eLife Assessment

This work reports an **important** new method for activity-dependent neuronal labeling in *Drosophila* using in situ hybridization, with the potential to establish a new standard in the field. The authors demonstrate the method's applicability by generating **compelling** evidence of the function of male-specific neurons in both aggression and courtship behaviors. These results and the new method will be of great interest to the neuroscience community.

https://doi.org/10.7554/eLife.92380.2.sa3

Introduction

Monitoring neuronal activity during specific actions or activities is critical to understanding how the brain controls behavior. Measurements within a local brain region of neural activity in non-transparent awake, behaving animals such as mice or fruit flies can be achieved with electrophysiological and calcium imaging techniques (Buzsáki, 2004; Grewe and Helmchen, 2009). In *Drosophila*, two-photon calcium imaging (TPI) has been widely used (Seelig et al., 2010) because single-unit electrical recording in the fly central brain remains exceedingly difficult (Turner et al., 2008; Wilson et al., 2004). But TPI in *Drosophila* requires head-fixation, which limits the repertoire of behaviors that flies can perform under these conditions. For example, it is difficult to use TPI to image neuronal activity during the consummatory phases of complex social behaviors, such as male-male aggression or male-female courtship (but see Clowney et al., 2015). Recently, a new method called Flyception2 was introduced for brain imaging in freely walking flies (Grover et al., 2020, 2016). However the spatial resolution of this method is limited, it is invasive, and monitoring the activity of single neurons in freely moving animals is still challenging.

In mice, immediate-early genes (IEGs) such as c-fos, Arc, or Egr1 have been used to map the activity of neurons by visualizing their expression histologically using immunohistochemistry (IHC) or in situ hybridization (ISH) (Morgan and Curran, 1991). More recently, this method has been combined with tissue-clearing and light-sheet microscopy to perform systematic and unbiased whole-brain mapping of neurons activated during different behaviors (Kim et al., 2015; Renier et al., 2016). An extension of this approach, called cellular compartment analysis of temporal activity by fluorescence in situ hybridization (catFISH), enables within-animal comparisons of neuronal populations activated during two different sequential behaviors (Guzowski et al., 1999; Lin et al., 2011).

In *Drosophila*, by contrast, the application of IEGs to map whole-brain neuronal activation patterns has been limited. In part this is because c-*fos* is not a particularly good activity marker in flies (Chen et al., 2016). More recently, several studies using fly IEGs such as *Hr38* and *stripe/Egr1* have been reported (Chen et al., 2016; Fujita et al., 2013; Takayanagi-Kiya et al., 2023; Takayanagi-Kiya and Kiya, 2019). Nevertheless, this technique has been relatively under-utilitized in flies. This may be the case, at least in part, because application of FISH to the adult *Drosophila* brain has been technically challenging, due to limited probe penetration and high background caused by traditional amplification methods such as Tyramide (Raap et al., 1995).

To circumvent these problems, we have applied in this study an *in situ* hybridization amplification technique called the Hybridization Chain Reaction (HCR), v.3.0 (Choi et al., 2018) to visualize the expression of *Hr38*, an IEG expressed by active neurons in the adult male fly brain (Fujita et al.,

2013). The design of HCR, which requires conjoint hybridization to target sequences of adjacent pairs of "half-probes" to achieve amplification, affords both greater sensitivity and specificity, allowing detection of low-abundance transcripts with minimal background noise and off-target hybridization. We call this approach HCR3.0-amplified IEG Fluorescent In Situ Hybridization, or "HI-FISH" (**Figure 1A**). Although we use *Hr38* as proof-of-concept, this approach is in principle applicable to any IEG.

Here we demonstrate three different applications of HI-FISH relevant to understanding the neural circuitry underlying social behaviors in flies. First, we have asked whether specific neuronal populations discovered in functional screens for aggression-promoting neurons (Asahina et al., 2014; Hoopfer et al., 2015; Watanabe et al., 2017) are indeed active during natural aggressive behavior, courtship or both. We have further investigated whether such activity is only observed during the contact-mediated consummatory phase of these behaviors, or can also be detected in freely moving flies in the absence of fighting or mating. Second, we have performed unbiased, whole-brain functional mapping of the downstream targets activated by optogenetic stimulation of a neuronal population of interest, a variant method we call "opto-HI-FISH.". We have applied this method to $P1^a$ neurons (Anderson, 2016; Clowney et al., 2015; Hoopfer et al., 2015; Inagaki et al., 2014) a subset of the male-specific P1 class of interneurons originally identified based on their ability to trigger male courtship behavior when stimulated (von Philipsborn et al., 2011). Finally, we have developed a variant of the catFISH technique (Guzowski et al., 1999), using dual-color FISH combining intronic and exonic *Hr38* probes, to compare neuronal populations activated during two different sequential behaviors, a method we call "HI-catFISH." Since experimental activation of $P1^a$ neurons can promote both aggression and courtship in pairs of male flies (Hoopfer et al., 2015), we have used HI-catFISH to investigate whether separate or overlapping subpopulations of $P1^a$ neurons are active during natural occurrences of these two social behaviors. Together, the results of these studies illustrate the utility of HI-FISH, opto-HI-FISH and HI-catFISH to detect the activation of both known and previously unidentified neurons during naturalistic social behaviors that are not amenable to head-fixation. The results have also yielded new biological insights into the neural circuit-level control of aggression and courtship.

Results

Brain-wide expression of *Hr38* detected by HI-FISH

The HCR3.0 method provides greater sensitivity, specificity and lower background than traditional FISH using Tyramide signal amplification (TSA). Application of older FISH methods in the *Drosophila* adult whole brain has been limited, due to low sensitivity and high background (Wilkie and Davis, 1998). For example, the detection by FISH of low-abundance transcripts such as those encoding GPCRs has been virtually impossible in adult flies up to now. Application of the HCR-FISH method, by contrast, was able to detect mRNA encoding an octopamine receptor Oct-TyrR (Arakawa et al., 1990; Saudou et al., 1990), as well as Dh44, a high-abundance neuropeptide-encoding transcript (Figure 1-figure supplement A and B) (Choi et al., 2018). Background in controls lacking the HCR initiator probes was essentially undetectable.

Next, we investigated the ability of HCR to detect brain-wide expression of *Hr38* following artificial (optogenetic) activation of fruitless-GAL4 (Stockinger et al., 2005) neurons expressing the red-shifted opsin Chrimson::tdT. Fru-GAL4 labels ~2,000 neurons in the adult male brain, providing a large number of potentially activatable cells. Following photostimulation *Hr38* signals were detected in virtually all Chrimson::tdT^+ neurons as well as in other tdT^- neurons (**Figure 1B, C** and Figure 1-figure supplement C). The latter may be indirectly activated via synaptic inputs from

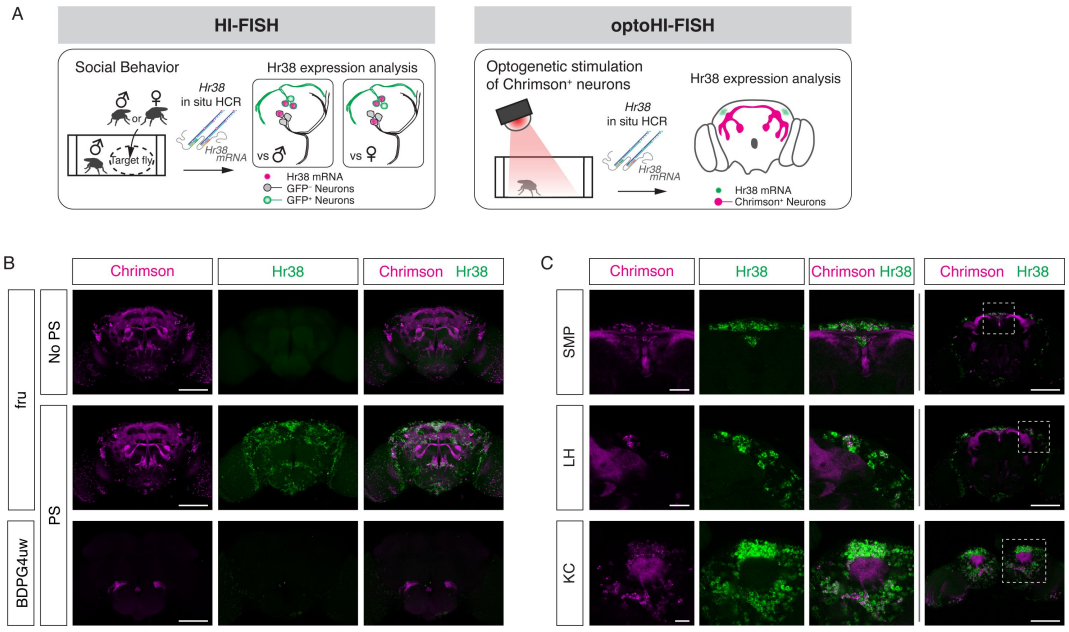

Figure 1.

Mapping neuronal activities using Hr38 FISH.

(A) Illustrated summary of this study for mapping Hr38 expression induced by social behavior or artificial activation of specific neuronal populations. (B) Representative images of Hr38 expression before (fru-No PS) and after photo-stimulation of fru-GAL4>Chrimson neurons (fru-PS). BDPG4uw-PS represents the images after Photo-stimulation of empty-GAL4>Chrimson neurons. magenta: Chrimson::tdT (native fluorescence), green: Hr38 HCR signals. Scale bar: 100μm. (C) Magnified confocal section images of Hr38 expression (left three columns) from the boxed region (far right column) after photo-stimulation of fru-GAL4>Chrimson neurons. SMP, superior medial protocerebrum; LH, lateral horn; KC, Kenyon cells. Scale bar: 20μm (left three columns) or 100μm (far right column).

Fru-GAL4^{+} neurons. Control flies of the same genotype but without photostimulation, or photostimulated flies with an "empty" GAL4 driver (BDPG4uw; Pfeiffer et al., 2008) displayed much lower levels of *Hr38* expression.

While performing these experiments, we observed that simply transferring flies to a new arena induced a significant level of *Hr38* expression throughout the brain (Figure 1-figure supplement D and E), likely reflecting the stress caused by the manipulation and new environment. Based on this observation, we conducted subsequent experiments after flies were habituated to the testing arena before starting the assays (see Methods). This minor modification proved essential to distinguishing behavior-specific HI-FISH signals from the widespread *Hr38* induction caused by transfer of the flies from their home vial to an experimental apparatus.

Mapping of neurons activated by social behaviors

As an initial proof-of-concept application of HI-FISH, we asked whether neuronal subsets initially identified in functional screens for aggression-promoting neurons (Asahina et al., 2014; Hoopfer et al., 2015; Watanabe et al., 2017) were actually active during natural aggressive behavior. These included P1^{a} (Hoopfer et al., 2015), Tachykinin-FruM^{+} (Tk^{FruM}) (Asahina et al., 2014) and aSP2 neurons (Watanabe et al., 2017). Despite the fact that activity in these neuron subsets was shown to be essential for normal aggression, it was formally possible that the behavioral phenotypes caused by their artificial stimulation were due to their supra-physiological activation. Therefore, we performed HI-FISH on fly lines carrying a myr:GFP reporter in the cell populations of interest in males paired with different types of target flies under different conditions. Thirty to 45 minutes after a 20 min interaction with the target fly, we fixed the brains and performed double-label HI-FISH together with fluorescent antibody staining of myr::GFP-expressing neurons (**Figure 1A**; see Methods).

In the control condition, where the experimental flies were kept alone during the observation period, there was little or no detectable *Hr38* expression in P1^{a}, Tk, or aSP2 neurons (**Figure 2A-D**, "Control"). In contrast, we observed clear *Hr38* signals in GFP^{+} P1^{a}, Tk, and aSP2 neurons after a male-male interaction that included fighting behavior (Aggression: **Figure 2A-D**, Figure 2-figure supplement. We also observed P1a-negative Hr38^{+} neurons neighboring P1a neurons during aggression (**Figure 2**, P1^{a} Hr38). These cells may correspond to other subpopulations of P1 neurons, or to Dsx-expressing pC1 neurons that have also been implicated in aggression (Koganezawa et al., 2016). Note that images are single confocal sections provided for qualitative, illustrative purposes only and should not be interpreted quantitatively. Our conclusions are based on statistically analyzed quantitative data presented in bar and box plots). In the case of courtship with a female, comparably strong *Hr38* induction was observed in P1^{a} and aSP2 neurons, while there was no *Hr38* expression in Tk neurons (**Figure 2A-D**, Figure 2-figure supplement; Courtship). These data are consistent with prior observations indicating that the functional manipulation of P1^{a} or aSP2 neurons in the male flies affects both male-male aggression and male-female courtship behavior (Hoopfer et al., 2015; Takayanagi-Kiya and Kiya, 2019; Watanabe et al., 2017), while the manipulation of Tk neurons affects only aggression (Asahina et al., 2014).

Social interactions in flies consist of multiple phases: approach, investigation, initial contact and progression to consummatory behaviors (Chiu et al., 2021; Yamamoto and Koganezawa, 2013). While electrophysiological recording or calcium imaging can identify neuronal activation that is time-locked to specific behavioral actions, the detection of *Hr38* (or any IEG) induction may reflect activation at any or all of these sequential phases due to the long-lived, accumulated expression of the IEG mRNA. To identify the phase(s) of social behavior wherein *Hr38* induction occurred, we separated the signals or interactions characteristic of these sequential phases in space rather than time. First, we asked whether the activation of these neurons during a male-male social interaction requires actual fighting behavior, or simply close contact with the target male. Initially, we paired the experimental male fly with a dead male, as a source of chemosensory cues. Because some male-derived cues (e.g., visual motion) may require a live conspecific, we also

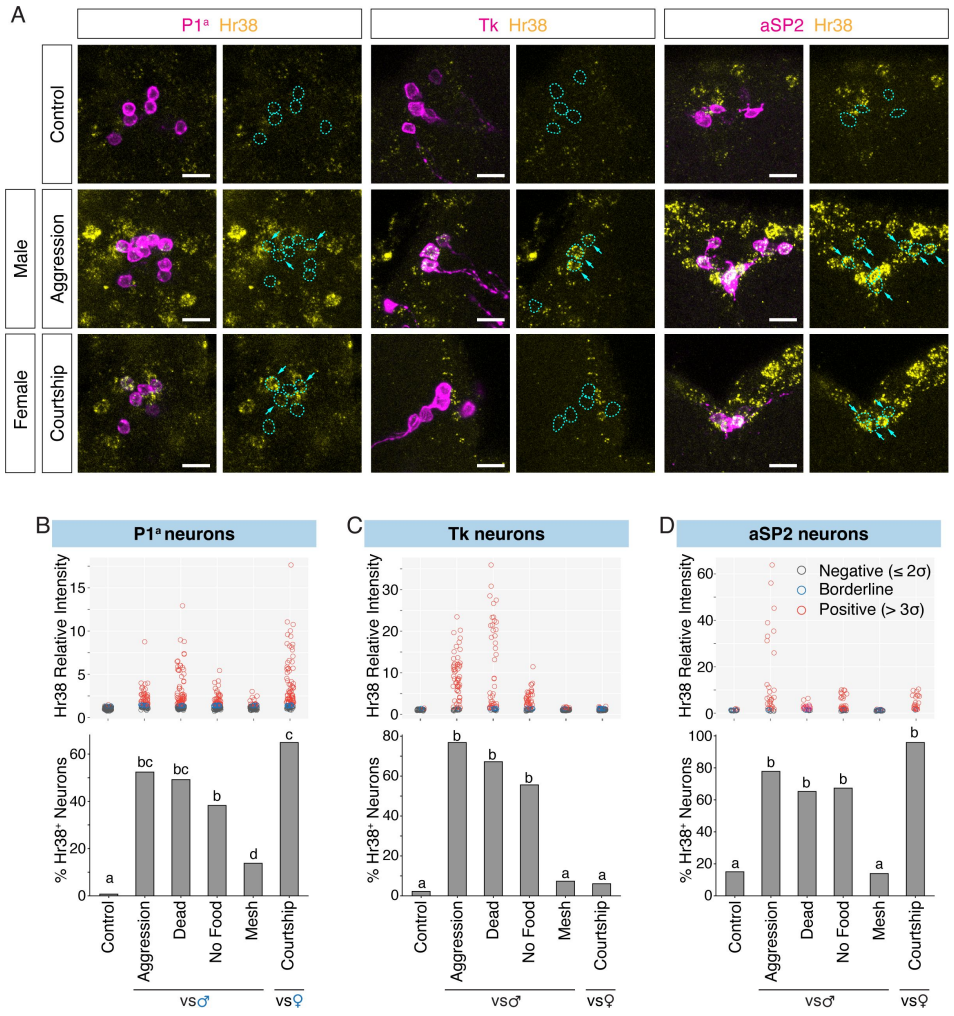

Figure 2.

Investigation of neurons activated by social behavior with Hr38 FISH.

(A) Hr38 expression in the neurons labeled with P1^a-split GAL4, Tk-GAL4, and aSP2-split GAL4 drivers. magenta: myr::GFP, yellow: Hr38 HCR signals. Dotted lines depicted the outlines of myr::GFP labeled cell bodies. Arrows: cell bodies of Hr38 positive neurons. Scale bar: 10μm. (B) (D) *Upper,* scatter plots indicate expression level (relative intensity) of Hr38 HCR signals; *lower* bar plots indicate percentage of Hr38 positive neurons ("positive" defined as neurons with a relative signal intensity > 3σ above the average signal intensity of the control condition) in P1^a (B), Tk (C), and aSP2 cells (D) after different behavioral episodes. Aggression: aggressive behavior against another male, Dead: interaction with a dead male, No Food: interaction with another male without food (no fighting), Mesh: interaction with another male, separated with mesh (no physical contact), Courtship: courtship behavior with a virgin female. Bar plots indicate the percentage of Hr38$^+$ neurons among GFP-labeled cells. Bars with the same letter are not statistically significantly different; bars with no common letter are significantly different ($p < 0.05$, chi-square test). Number of neurons and individuals analyzed; P1^a-Control: 135 (N = 8), P1^a-Aggression: 84 (N = 5), P1^a-Dead Male: 126 (N = 7), P1^a-No Food: 115 (N = 6), P1^a-Mesh: 87 (N = 6), P1^a-Courtship: 114 (N = 6), Tk-Control: 45 (N = 4), Tk-Aggression: 69 (N = 6), Tk-Dead Male: 61 (N = 6), Tk-No Food: 63 (N = 6), Tk-Mesh: 82 (N = 8), Tk-Courtship: 66 (N = 6), aSP2-Control: 20 (N = 3), aSP2-Aggression: 36 (N = 4), aSP2-Dead Male: 23 (N = 3), aSP2-No Food: 49 (N = 4), aSP2-Mesh: 36 (N = 4), aSP2-Courtship: 24 (N = 3).

placed the experimental and tester males in an arena with an agarose substrate. Under these conditions, physical contact but not fighting occurs (Lim et al., 2014). In both "touching but no fighting" conditions, the fraction of Hr38^{+} cells among P1^{a}, Tk and aSP2 neurons was slightly lower but not statistically significantly different from that measured during actual aggression, while the intensity of *Hr38* mRNA expression in positive cells was slightly lower in the No Food condition (Dead Male and No Food: **Figure 2B-D**, Figure 2-figure supplement). Thus the activation of P1^{a}, Tk, or aSP2 neurons does not require consummatory aggressive actions such as lunging, tussling or boxing (Chen et al., 2002).

Interacting male flies can, in principle, exchange visual, auditory, mechanosensory or chemosensory cues. In the case of chemosensory signals, inter-male aggression has been shown to require both detection of volatile cues by the olfactory system, and of non-volatile cues by the gustatory system (Fernández and Kravitz, 2014; Wang et al., 2011; Wang and Anderson, 2010). While both types of cues are present when an experimental fly is exposed to an intact or a dead male fly, the detection of non-volatile cues requires contact chemosensation (Vosshall and Stocker, 2007). We therefore exposed the experimental males to a target fly separated by a mesh filter which prevented physical contact between the freely moving flies. Interestingly, *Hr38* induction in all 3 cell populations under this condition was significantly weaker that that measured during free interaction with a male on agarose, where contact but no fighting occurred (Mesh: **Figure 2B-D**, Figure 2-figure supplement). Taken together with the relatively strong *Hr38* induction observed following contact with a dead male (which presumably provide a source of both olfactory and gustatory pheromones), these data suggest that strong activation of P1^{a}, Tk, and aSP2 neurons requires the integration of both volatile and non-volatile male-derived chemosensory cues. However the results do not exclude the possibility that these neurons exhibit additional activity during contact-mediated aggression, but which is not statistically detectable by this method in comparison to "no fighting" controls.

Detection of *Hr38*$^{+}$ cells induced by optogenetic stimulation of P1^{a} neurons in the male brain

Optogenetic and thermogenetic stimulation experiments have shown that P1^{a} interneurons can promote both male-directed aggression and male- or female-directed courtship (Hoopfer et al., 2015; von Philipsborn et al., 2011). While the neural circuitry downstream of P1 neurons that promotes female-directed courtship behavior has been well-characterized (von Philipsborn et al., 2011), the pathway by which P1^{a} neurons can promote aggression is poorly understood. As a first step to identify systematically P1^{a} functional downstream targets, we optogenetically activated P1^{a} neurons using Chrimson:tdT and mapped the brain-wide pattern of *Hr38* induction in males (**Figure 3A-D**), a method we call "opto-HI-FISH (**Figure 1A**)." To analyze these data, images of *Hr38* expression from multiple individuals were registered to a reference brain using antibody labeling of Bruchpilot (Brp), a reference neuropil marker, to generate an average induction pattern (**Figure 3E**) (Cachero et al., 2010). We then created a voxel-based heat map for the *Hr38* expression from the average image. The heat map indicated that neurons around the posterior dorsal region of the central brain were strongly activated by P1^{a} stimulation (**Figure 3F**).

To validate this approach, we first asked whether we could detect *Hr38* induction in pCd neurons, which were previously shown by calcium imaging to be (indirect) targets of P1^{a} neurons (Jung et al., 2020). Double-labeling in pCd-GAL4; UAS-GFP flies using HI-FISH and immunostaining for GFP (see Methods) confirmed that *Hr38* was strongly induced in pCd neurons by P1^{a} photostimulation (**Figure 3G**, pCd). Next, we asked whether we could identify any of the specific cellular targets of P1^{a} neurons in brain regions that exhibited strong induction of *Hr38*. These regions included Kenyon cells (KCs) and PAM dopaminergic neurons in the mushroom body (MB; **Figure 3F**). We used the GAL4 drivers OK107 (Connolly et al., 1996) to label KCs, and 0273 and Ddc-GAL4 to label PAM neurons. Following P1^{a} optogenetic activation, brains were processed for

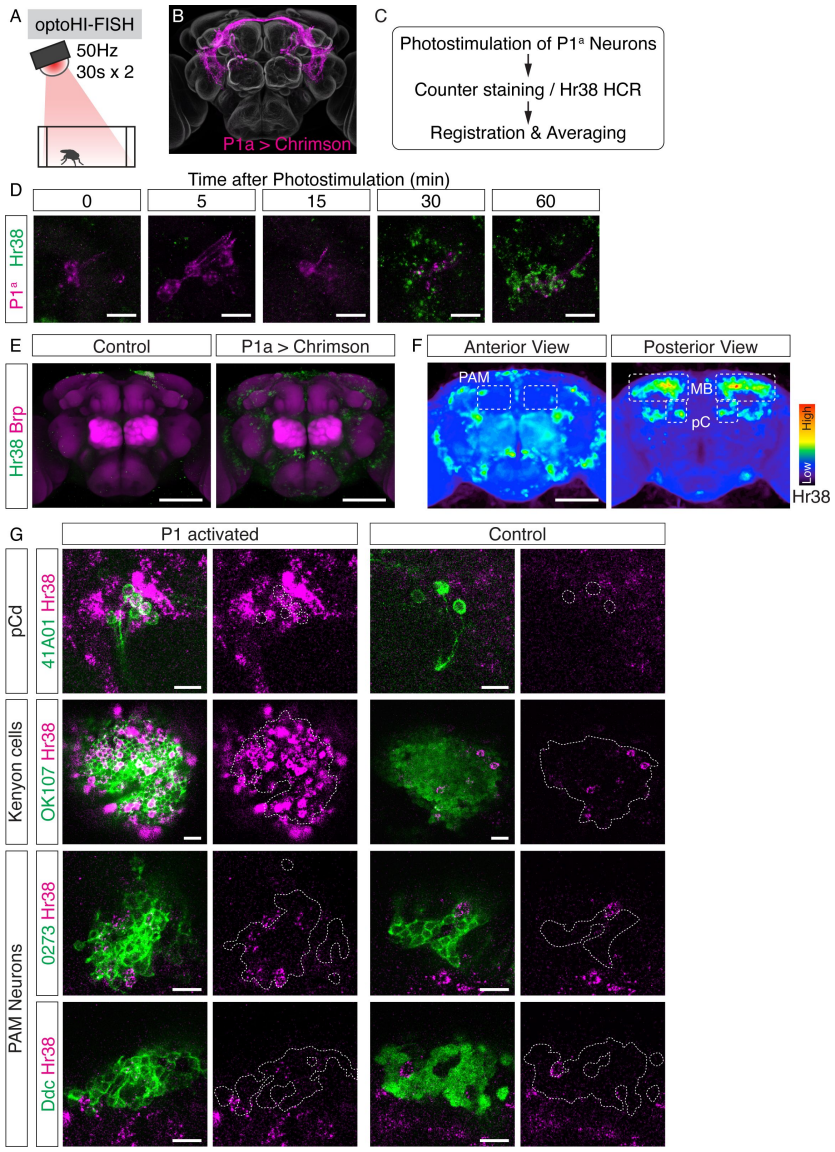

Figure 3.

Investigation of downstream neurons activated by optogenetic activation of P1^{a} neurons.

(A) Illustration of the experimental set up. (B) Expression pattern of Chrimson::tdT driven by P1^{a} split GAL4. (C) Scheme of the data analysis procedure. (D) Time-course study of Hr38 HCR expression after P1^{a} photo-stimulation in P1^{a} labeled neurons and the surrounding area. By 30-60 mins, most of the P1^{a} labeled neurons expressed Hr38 (96.8% of P1a labeled neurons at 30 min). Scale bars: 10μm. (E) Average image of Hr38 expression of control (BDPG4Uw) and P1^{a}-activated brains. 5 individual brains from each conditions were registered into a template brain and averaged. Green: Hr38 HCR signals, Magenta: Brp. Scale bar: 100μm. (F) Heat map analysis of Hr38 expression. Areas depicted by dotted lines represent the areas of PAM neurons (PAM), mushroom bodies (MB), and pC neurons (pC). Scale bar: 100μm. (G) Confocal images of Hr38 expressions in pCd neurons (R41A01), Kenyon cells (OK107), and PAM neurons (0273 or Ddc) of control and P1^{a} activated brains. Green: myr::GFP, Magenta: Hr38. Dotted lines depicted the outlines of cell bodies (pCd) or cluster of neurons (KC, PAM). Scale bar: 10μm.

double-labeling with HI-FISH and anti-GFP antibody staining to identify the cells of interest. We observed evidence of *Hr38* induction in all three cell populations, although the signal was difficult to quantify due to the high density of GFP^+ cells (**Figure 3G**).

To confirm the results of the opto-HI-FISH experiments, we next asked whether PAM neurons and/or Kenyon cells were activated in response to $P1^a$ stimulation using *in vivo* calcium imaging in living, head-fixed flies. We expressed a calcium indicator, jGCaMP7b (Dana et al., 2019) in either Kenyon cells or PAM neurons using the GAL4/UAS system and Chrimson::tdT in $P1^a$ neurons using the LexA/LexAop system (Brand and Perrimon, 1993; Lai and Lee, 2006). The neurites of both KCs and PAM neurons showed significant time-locked responses to optogenetic activation of $P1^a$ neurons (Figure3-figure supplement 3A-F). We also imaged jGCaMP7b signals from cell bodies of PAM neurons while photo-stimulating $P1^a$ neurons, and observed clear responses in both cases as well (Figure 3-figure supplement 3G-J). Although we could not identify the specific activated cell populations among the KCs (data not shown), $P1^a$ photo-stimulation evoked a significant rise in $\Delta F/F$ in ~50 % of PAM neurons (Figure 3-figure supplement 3I). These data validate the results from brain-wide *Hr38* induction mapping and provide proof-of-concept that brain regions containing functional targets of a cell population of interest (here $P1^a$ neurons), as well as specific neuron subtype targets within these regions (KCs and PAM neurons), can be identified by opto-HI-FISH. These results are also consistent with a recent report showing that subsets of PAM dopaminergic neurons receive excitatory inputs from P1 neurons, and assign to KCs a positive valence associated with P1 activation (Shen et al., 2023)

HI-catFISH reveals distinct fighting- and mating-activated $P1^a$ neuron subsets

Previous reports showed that artificial activation of $P1^a$ neurons promoted both aggression and courtship. The foregoing data indicated that *Hr38* was induced in $P1^a$ neurons after both natural aggressive and courtship behavior (**Figure 2**, Figure 2-figure supplement). An important outstanding question is whether the aggression-and courtship-activated $P1^a$ populations are the same or different (Anderson, 2016). Because individual P1 neuron subtypes cannot be distinguished by FISH, between-animal comparisons of *Hr38* induction following fighting or mating cannot distinguish these two possibilities. To compare directly which $P1^a$ neurons are active during naturalistic mating vs. aggression, we developed an *Hr38* analog of catFISH (HI-catFISH) to compare neurons activated during aggression and courtship in the same animal (**Figure 4A**). The catFISH method exploits the different kinetics of nuclear-cytoplasmic transport and of IEG mRNA stability (Guzowski et al., 1999) to distinguish neurons activated during a behavior performed just prior to analysis (nuclear pre-mRNA), from those activated during a different behavior performed 30 min before the second (cytoplasmic mRNA); cells activated during both behaviors contain both cytoplasmic and nuclear signals (**Figure 4B**). In mice, we have used catFISH with c-*fos* to compare hypothalamic neurons activated during aggression vs. mating in males (Lin et al., 2011).

We detected neuronal populations activated during two consecutive social behaviors using HI-FISH containing *Hr38* intronic and exonic probes amplified using different fluorophores. In two color FISH, unspliced pre-mRNAs were detected as nuclear dots labeled by both probes, while mRNA was detected as a more diffuse cytoplasmic signal detected by only the exonic probe (**Figure 4B**). A time course study using opto-HI-FISH with these two different *Hr38* probes indicated that the primary RNA transcripts first appeared in $P1^a$ nuclei ≤15 min after optogenetic activation, and disappeared by 60 min. Conversely, cytoplasmic processed mRNAs started to accumulate in the cytoplasm 30 min after activation and disappeared by 2-3 hours after stimulation (Figure 4-figure supplement A-C).

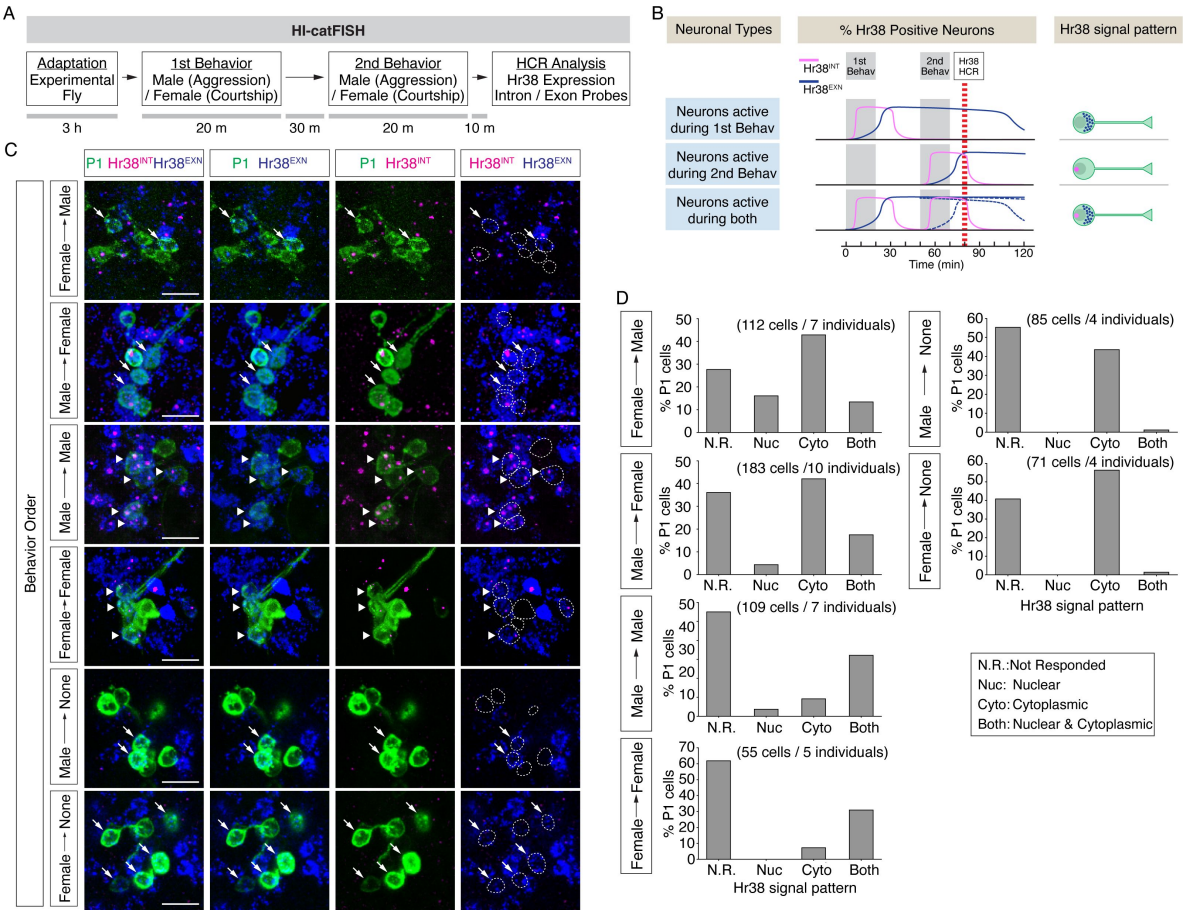

Figure 4.

Drosophila catFISH reveals P1[a] subpopulations activated by two different social behaviors.

(A) Experimental design of the fly catFISH. Each fly experienced the 1st behavior (aggression or courtship) followed by 2nd behavior (aggression or courtship), and the HCR was performed with the Hr38 probes targeted for the exon or the intron sequence. (B) Time-course of Hr38 signals detected by the exon- or the intron-targeted Hr38 HCR probes and expected Hr38 signals in each neurons. (Top) The intron-targeted Hr38 HCR signals (magenta) induced by 1st behavior disappear at the timing of HCR analysis while the exon-targeted Hr38 signals (blue) remain in the cytoplasmic area. (Middle) Both intron-targeted and exon-targeted signals are present in the nucleus. (Bottom) Both intron-targeted and exon-targeted signals induced by the 2nd behavior are present in the nucleus, and exon-targeted Hr38 signals induced by the 1st behavior are present in the cytoplasmic area. In 'Neurons active during both', the exon probe signals from the 1st behavior decline (dotted blue line *1) after 60 mins (also see Fig. 4B-supplement). However, it is canceled out as the signals from 2nd behavior are increased (dotted blue line *2). As a result, the combined Hr38 exon probe signals (solid blue line) remain high at the time point for Hr38 HCR. (C) Representative images of Hr38 HCR signals in P1[a] neurons after six different behavioral conditions. Green: myr::GFP, Magenta: intron-targeted Hr38 HCR signals: exon-targeted Hr38 signals. Scale bar: 10μm. The images shown are for illustration purposes only and represent single optical sections covering only a portion of the P1[a] neuronal cluster. They exclude P1[a] cells present in other Z-planes. Quantification (D) was based on signals measured in all P1[a] cells contained within an entire Z-stack. See also Figure 4 - figure supplement D. (D) Fraction of responsive P1[a] neurons across indicated conditions. N.R.: not responded, Nuc: nuclear signal only (responded to only second target), Cyto: cytoplasmic signal only (responded to only first target), Both: nuclear and cytoplasmic signal (responded to both first and second target).

Having established this calibration of the temporal resolution of HI-catFISH, we compared labeling during free social interactions with a male or a female target. Following pre-habituation (see above), a naïve experimental male fly was placed into a behavioral arena, and a male or female fly was introduced as a first target. After 20 minutes of free social interactions the target fly was removed from the arena and, after a further 30 min recovery period, replaced by a second target fly (male or female; Methods). All four combinations of sex of the 1st and 2nd target fly, and two additional control conditions, in which the experimental flies were exposed to only the 1st target fly (Male -> None, Female -> None), were tested (**Fig. 4C**). For the two sequential behaviors condition, ten minutes after exposure to the second target fly (and ~1 hr after exposure to the first target fly), the experimental fly was sacrificed and analyzed by dual-color HI-FISH *Hr38* (**Figure 4A and B**).

As expected, many of the neurons activated by the first target were re-activated by the second target (nuclear and cytoplasmic signal), when the sex of the two target flies was the same (**Figure 4C**, Male -> Male, Female -> Female, arrowheads and **Figure 4D**, "Both" vs. "Cyto"). In contrast, few neurons exhibited nuclear Hr38 transcripts detected with the intronic probe when the experimental flies were exposed to the only 1st target fly but sacrificed after an additional 60 minutes (**Figure 4C**, Male -> None, Female -> None, "Nuc" or "Both"). By contrast, many neurons activated by the first target fly (cytoplasmic signal) were not activated by the second target fly (nuclear signal), when the target sexes were different (**Figure 4C**, Female -> Male, Male -> Female, arrows and **Figure 4D**, "Cyto" vs. "Both"). Responses to males were clearly detected in a subset of P1^{a} neurons whether the male was presented first (**Figure 4C**, Male → Female; GFP^{+}; dashed oval outlines containing blue diffuse cytoplasmic signal) or second (**Figure 4C**, Female → Male; magenta nuclear dots). In addition, there were male-activated cells nearby that were not labeled by the P1^{a}-split GAL4 driver. In general, these male HI-FISH signals did not overlap with the HI-FISH signals evoked by female targets. (We note, however, that relatively few neurons were activated by the female fly when the sex of the two targets was different, regardless of whether the female was presented first or second; the reasons for this are currently unclear but may reflect a suppressive effect of aggression neuron activation on courtship neuron activity, as suggested by earlier studies (Hoopfer et al., 2015).) These data suggest that there may be distinct P1^{a} subpopulations that are activated during either male-male aggression or male-female courtship.

Discussion

Drosophila is a powerful model system for identifying and characterizing neural circuits that control innate behaviors. With recent progress in two-photon imaging techniques using genetically encoded calcium sensors, it has become possible to monitor activity from genetically labeled neurons at single-cell resolution in head-fixed flies (Seelig et al., 2010). Although single-neuron imaging in unrestrained behaving animals has been achieved in mammalian studies (Flusberg et al., 2008; Remedios et al., 2017; Ziv et al., 2013) most imaging studies with single-cell resolution in *Drosophila* require head-fixed conditions. Therefore, the repertoire of naturalistic behaviors that can studied using this approach – in particular social behaviors dependent on chemosensory cues (but see Hindmarsh Sten et al., 2021)– remains limited.

In mammalian systems, the discovery that IEGs such as c-*fos* are induced by neuronal activity (Greenberg et al., 1985; Greenberg and Ziff, 1984) has enabled brain-wide functional mapping of neuronal activation following specific behaviors (Morgan and Curran, 1991; Renier et al., 2016). This method and its derivatives have had a transformative impact on the identification of behaviorally relevant neural circuits in rodents. In *Drosophila*, by contrast, few if any studies describe the application of IEGs for brain-wide activity mapping. In this report, we applied the HCR3.0 RNA-FISH technique (Choi et al., 2018) to visualize the expression of a fly IEG, *Hr38* in the entire adult male brain following different manipulations (see also Shao et al., 2019). We

present data providing proof-of-concept that HI-FISH can be used to detect the activation by naturalistic stimuli of neurons previously identified in thermogenetic behavioral activation screens, as well as to identify candidate downstream targets of these neurons following their optogenetic activation (opto-HI-FISH). We also compared neuronal subsets within a small identified population ($P1^a$ neurons) that is activated during two different social behaviors, using HI-catFISH.

Monitoring Neuronal Activities during Social Behaviors

Previous studies reported that male-specific $P1^a$, Tk, and aSP2 neurons promote male-male aggression (Asahina et al., 2014; Hoopfer et al., 2015; Watanabe et al., 2017). In addition, $P1^a$ and aSP2 neurons promote male-female courtship (Hoopfer et al., 2015; Takayanagi-Kiya and Kiya, 2019). Artificial manipulation of the activity of these neurons affected social behaviors and demonstrated their causal roles in these behaviors. However, there was no direct evidence showing that these neurons are normally activated during the specific behaviors they can promote.

Our HI-FISH data demonstrated that $P1^a$ and aSP2 neurons are active during male-male aggression and male-female courtship, consistent with the behavioral effects of activating these neurons (**Figure 2**) (Hoopfer et al., 2015; Watanabe et al., 2017). In contrast, Tk^{FruM} neurons were only active during male-male aggression (**Figure 2**), consistent with their lack of a functional role in courtship (Asahina et al., 2014). Furthermore, we show that $P1^a$, Tk, and aSP2 neurons can apparently be activated by chemosensory cues from an opponent male fly in the absence of attack behavior (**Figure 2**). These data suggest that $P1^a$, Tk, and aSP2 neurons may serve to process and integrate sensory cues from the opponent and relay that information to the downstream neurons that encode the consummatory phase of aggression (Chiu et al., 2021). However they do not exclude that these neurons may play a role during overt attack.

Although the time resolution of IEG-based activity monitoring falls far short of that of calcium imaging, our data show that one can nevertheless use HI-FISH to separate activation that occurs during the appetitive vs. consummatory phases of male-male aggression, by judicious manipulation of experimental conditions.

Identification of downstream target neurons of genetically labeled neurons by opto-HI-FISH

Artificial activation of $P1^a$ neurons induces male-female courtship and an internal state that promotes male-male aggression (Bath et al., 2014; Hoopfer et al., 2015; Inagaki et al., 2014). Furthermore, artificial activation of male specific P1 neurons mimics courtship-induced place preference as well as supporting appetitive olfactory conditioning (Shen et al., 2023). It is critical to identify neurons that are functionally downstream of $P1^a$ cells to understand how these neurons can promote this state. In this study, using opto-HI-FISH we identified pCd neurons, Kenyon cells and PAM neurons as downstream targets of $P1^a$ neurons. These results were confirmed by two-photon calcium imaging analysis (**Figure 3**, Figure 3-figure supplement). Importantly, recent studies have reached the same conclusions regarding neuronal populations using different approaches (Jung et al., 2020; Shen et al., 2023). These findings provide additional support for our methodology. The heat map illustrates the presence of additional potential $P1^a$ -follower populations beyond the three interrogated here (**Figure 3F**). Further analysis will unveil the detailed characteristics of these potential downstream neurons of $P1^a$ neurons. An important caveat is that not all active *Drosophila* neurons may express *Hr38*. Act-seq data from mice indicates that different neuron subsets activated during social behaviors express different IEGs to different extents (Kim et al., 2019).

Functional heterogeneity of P1^a populations during Social Behaviors

In addition to identifying functional downstream targets of P1^a neurons, characterizing cellular diversity among P1^a neurons and how this functional heterogeneity maps onto their connectivity with different downstream targets is critical to understanding how these cells can induce both courtship and aggressive behavior. Optogenetic activation of P1^a neurons at a low frequency promotes aggression towards males, while high-frequency stimulation promotes male-directed courtship during stimulation, followed by aggression in the inter-stimulation intervals (Hoopfer et al., 2015). P1^a neurons may control these two behaviors according to their activity level and/or the subtype of neuron activated in the population. Alternatively, P1^a neurons may indirectly promote fighting by inhibiting aggression-promoting neurons during courtship (Koganezawa et al., 2016); post-inhibitory rebound in such neurons following the offset of P1^a optogenetic stimulation may trigger aggressive behavior (Anderson, 2016).

Our preliminary *Hr38* catFISH results suggest the presence of male- or female-responsive subsets within the P1^a population, which consists of 8-10 neurons/hemibrain (**Figure 4**). To our knowledge, this is the first evidence that P1^a neurons are activated during male-male social interactions. Previous studies using calcium imaging of head-fixed flies suggested that P1^a neurons were inhibited by the male-specific pheromone, 11-cis-vaccenyl acetate (cVA; Clowney et al., 2015). The reason for this apparent discrepancy is not yet clear. The molecular identity of the male- vs. female-responsive P1^a subsets remains to be determined. It has been suggested that FruM$^+$ P1 neurons exclusively control courtship, while Dsx$^+$ P1 neurons (also called pC1 neurons; Koganezawa et al., 2016)) control aggression. However triple-intersection experiments have demonstrated that thermogenetic (Hoopfer et al., 2015) or optogenetic (Watanabe et al., 2017) activation of FruM$^+$ P1^a neurons, which comprise only 1-4 neurons/hemibrain, can also promote aggression. Therefore, while our results support the idea that different P1 subsets control aggression vs. courtship, they do not support the view that FruM$^+$ P1 neurons only control the latter and not the former social behavior.

While this paper was in the final stages of preparation, a manuscript by Takayanagi-Kiya et al. appeared that described a method for labeling neurons activated during innate behaviors using a different immediate early gene, *stripe/egr-1* (Takayanagi-Kiya et al., 2023). To analyze neuronal activities in different behavioral contexts, that study utilized a GAL4 driver for the *stripe/egr-1* gene to label neurons activated by the first behavior and immunostaining for stripe protein to label the second behavior. The flies were exposed to the first target for 24 hours, followed by exposure to the second target for 2 hours. In contrast, our approach for HI-catFISH is based purely on detecting the expression of the IEG mRNA using a state-of-the-art amplification method, HCR v3.0 (Figure 1-figure supplement B) (Choi et al., 2018). This enables us to monitor neuronal activity during two different behaviors with much higher temporal resolution than the analogous method of Takayanagi-Kiya. Furthermore, by combining our HI-catFISH with their protein expression-based method, it is theoretically possible to monitor neurons activated by four different behavioral contexts. Thus, the two methods complement each other.

In mice, distinct subpopulations of estrogen receptor 1 (Esr1)-expressing neurons in the ventrolateral subdivision of the ventromedial hypothalamus (VMHvl) are activated during male-directed aggression versus female-directed mating (Karigo et al., 2021; Remedios et al., 2017). Our observation that apparently distinct subpopulations of P1^a neurons are activated during aggression versus courtship in *Drosophila* strengthens the analogy between these two control nodes for social behavior (Anderson, 2016). Application to P1^a neurons of Act-Seq, a method that uses scRNAseq to identify transcriptomic cell types that are active during different behaviors as determined by IEG expression (Kim et al., 2019; Wu et al., 2017), may help to identify transcriptomic and functional diversity within the P1^a population. Such correlative studies may be

extended to functional perturbations by using transcriptomic data to identify more specific intersectional GAL4 drivers for distinct P1[a] subsets. Together, our studies illustrate how HI-FISH can provide a systematic, unbiased and brain-wide approach to identifying entry points to circuits controlling specific social behaviors, which can be integrated eventually with imaging, connectomic, transcriptomic and functional approaches to circuit analysis.

Materials and methods

Fly stocks

A list of the full genotypes for the flies used in this research is in Supplementary file 1.

R15A01-iLexA (improved LexA) was generated for this study. Briefly, the R15A01 enhancer fragment (Jenett et al., 2012) was cloned into pBPnlsLexA::p65::GADUw (Chiu et al., 2021).

20xUAS-IVS-Syn21-Chrimson::tdTomato3.1 (attP2) and 13xLexAop2-IVS-Syn21-Chrimson::tdTomato3.1 (su(Hw)attP5) were obtained from G. Rubin (Janelia Research Campus). 0273-GAL4 (Burke et al., 2012) was obtained from S. Waddell (The University of Oxford). fru^{GAL4} (Stockinger et al., 2005) was from B. Dickson (Janelia Research Campus).

The following strains were obtained from Bloomington Drosophila Stock Center (Indiana University); R15A01-AD (attP40), R71G01-DBD (attP2), R41A01-GAL4 (attP2), OK107, Ddc-GAL4, 20xUAS-IVS-jGCaMP7b (VK00005).

Optogenetic activation in behaving flies

A detailed description of the setup used for optogenetic activation was described previously (Inagaki et al., 2014; Watanabe et al., 2017). Flies were raised at 25°C and collected on the day of eclosion and kept in the dark for 7-10 days on the fly media containing 0.4 mM all *trans*-Retinal (Merck, St. Louis, MO). The experiments were performed with the “8-well” chamber (16 mm diameter x 10 mm height) with IR backlight. (855 nm, SOBL-6x4-850, SmartVision Lights, Norton Shores, MI). A 655 nm 10 mm Square LED (Luxeon Star LEDs Quadica Developments, Brantford, Canada) was used for photostimulation. The stimulation protocols for each experiment are described in the figures or figure legends.

Behavioral Assays

Flies were maintained at 9AM:9PM Light:Dark cycle. For male-male aggression assays and male-female courtship assays, the “8-well” acrylic chamber was used as described previously (Inagaki et al., 2014; Watanabe et al., 2017). The walls of the chamber were coated with a fluoropolymer resin (PTFE-30, Insect-a-Slip) (BioQuip Products, Rancho Dominguez, CA). The clear top ceiling plate was coated with Sigmacote (Merck, St. Louis, MO) to prevent flies from walking on the surfaces. The floor was covered with a layer of apple juice/sucrose-agarose food. The arena was illuminated with IR backlighting.

Two-photon calcium imaging

Calcium imaging with optogenetic activation was performed as described (Inagaki et al., 2014; Jung et al., 2020). A deep red (660 nm) fiber-coupled LED (Thorlabs, Newton, NJ) with a band-pass filter (660 nm, Edmund Optics, Barrington, NJ) was used for light source to activate Chrimson.

Flies were collected on the day of eclosion and kept in the dark on the fly media containing 0.4 mM all *trans*-Retinal (Merck, St. Louis, MO). 7-10 days old flies were cold-anesthetized using a temperature-controlled stage and mounted on a plastic plate with a small window using wax. The

cuticle of the dorsal side of the head was removed by forceps. Flies were then placed beneath the objective.

Fly saline (108 mM NaCl, 5 mM KCl, 4 mM $NaHCO_3$, 1 mM NaH_2PO_4, 5 mM trehalose, 10 mM sucrose, 5 mM HEPES, 0.5 mM $CaCl_2$, 2 mM $MgCl_2$, pH = 7.5) was used to bathe the brain during imaging.

Immunohistochemistry and HCR fluorescence in situ hybridization (FISH)

In situ HCR was performed as previously described with minor modifications (Choi et al., 2018, also see *https://www.moleculartechnologies.org/supp/HCRv3_protocol_generic_solution.pdf*). For the hybridization buffer, formamide was substituted with an equal volume of 8M urea solution for better preservation of tissue morphology (Sinigaglia et al., 2018).

To process multiple individuals, we collected flies (~ 8 individuals at once), soaked them in ice-cold ethanol to remove the wax on the cuticle, and opened the head cuticle of each fly with minimal time-lag among samples in the ice-cold fixative (4% paraformaldehyde in PBS). After brief fixation, the brain from each individual was dissected and fixed for 2 hours at 4℃.

For combination of immunohistochemistry (IHC) and HCR FISH, we performed IHC as described previously before HCR FISH procedure in RNase free condition (Watanabe et al., 2017). For antibody incubation, we added RNasin Plus (5% of final volume, Promega, Madison, WI). After immunostaining, the samples were post-fixed with 4% formaldehyde in PBS and proceeded for HCR. HCR probes were purchased from Molecular Technologies (*https://www.moleculartechnologies.org/*). The identifiers for each probes are as follows; Hr38 (exon): Hr38_MT 2627/B655 (B2 Amplifier) and Hr38 3278/C629 (B5 Amplifier), Hr38 (intron): HR38intron 3736/D801 (B1 Amplifier), Dh44: Dh44 3174/C241 (B3 Amplifier), Oct-TyrR: Oct-TyrR_CDS 3008/B815 (B2 Amplifier). We tested two different Hr38 probes (2627/B655 and 3278/C629) and obtained the same results. Images of HCR3.0 data presented in this manuscript were obtained using the Hr38_MT 2627/B655 probe set. The samples were mounted in 88% (w/v) Histodenz in 0.02 M Phosphate buffer (pH 7.5 with NaOH) with 0.1% Tween-20 and 0.01% sodium azide (Yang et al., 2014).

The antibodies used were as follows: rat anti-DN Cadherin (1:50, DN-EX #8, developed by T. Uemura, obtained from Developmental Studies Hybridoma Bank, University of Iowa, Iowa City, IA), mouse anti-Bruchpilot (1:50, nc82, developed by E. Buchner, obtained from Developmental Studies Hybridoma Bank, University of Iowa, Iowa City, IA), rabbit anti-GFP (1:1,000, A11122, Thermo Fisher Scientific, Waltham, MA), Goat anti-Mouse IgG (H+L) Alexa Fluor 488 (1:1,000, A-11001, Thermo Fisher Scientific, Waltham, MA), Goat anti-Mouse IgG (H+L) Alexa Fluor 568 (1:1,000, A-11004, Thermo Fisher Scientific, Waltham, MA), Goat anti-Mouse IgG (H+L) Alexa Fluor 633 (1:1,000, A-21050, Thermo Fisher Scientific, Waltham, MA), Goat anti-Rabbit IgG (H+L) Alexa Fluor 488 (1:1,000, A-11008, Thermo Fisher Scientific, Waltham, MA), Goat anti-Rabbit IgG (H+L) Alexa Fluor 488 (1:1,000, A-11011, Thermo Fisher Scientific, Waltham, MA), Goat anti-Rabbit IgG (H+L) Alexa Fluor 633 (1:1,000, A-21070, Thermo Fisher Scientific, Waltham, MA)

Confocal serial optical sections were obtained with a Fluoview FV3000 Confocal Microscope (Olympus, Tokyo, Japan).

For the Hr38 exonic probe, we first measured average fluorescence intensity within the cell boundary using Fiji (Schindelin et al., 2012; Schneider et al., 2012) and calculated the relative intensity to the background signals and then defined the positive cells whose signals were above 3σ. For each optical section we defined as the background signal the area outside the region with clearly $Hr38^+$ cells, because the intensity of the background signal varies depending on the depth of the optical section.

For image registration, brain images were registered to T1 template brain (Yu et al., 2010) using the CMTK registration plugin of Fiji (*https://flybrain.mrc-lmb.cam.ac.uk/dokuwiki/doku.php?id=warping_manual:registration_gui*). To create average images for each condition, MATLAB was used to generate averaged images of each z-plane from different individuals. For voxel-based heat map analysis of the *Hr38* expression, the median filter (pixel size = 10) in Fiji was applied to the averaged images. Fiji and Fluorender software (Yong Wan et al., 2009) were used to create z stack images.

catFISH

To prepare target flies, 4 to 6 particles of small iron filings (Delta Education, #060-0313 or equivalent) were attached on the dorsal side of the thorax of 6-8 days old male or female flies using UV-activated glue under CO_2 anesthesia one day before the experiment. This allowed us to remove the target fly from a behavioral arena through a small hole using a neodymium magnet.

6-8 days single-housed male flies were used for the experimental flies. A male fly was introduced in the behavioral arena and allowed to habituated to the new environment for ~ 3 hours. The first target fly was introduced into the arena, and the experimental fly was exposed to the target for 20 mins. After the exposure, the target fly was removed from the arena as describe above. The experimental fly was given a 30-min interval before the second target was introduced. After 20 min exposure, the second target was removed, and *Hr38* expression was analyzed 10 min after the target fly removal (**Figure 4A and B**). Neurons were considered as positive for the Hr38 intronic probe when a clear dot signal with the intronic probe that co-localized with the Hr38 exonic signal was observed.

Statistical Analysis

Statistical analyses were performed using MATLAB (MathWorks, Natick, MA) and Python (Python Software Foundation). The detailed information including the number of samples, the statistical method, and the p value for each experiment is indicated in the figure legends.

Calcium imaging data analysis

T-series images were manually screened and omitted from further analysis in cases where images were shifted in Z-direction, indicative of Z-motion artifacts. For image registration on the X-Y axis, T-series images were opened in Fiji by importing as Image Sequences. The Template Matching Plugin was used for motion correction. Briefly, from the Plugins menu, we selected Template Matching, then selected Align Slices in Stack. We then selected Normalized Correlation Coefficient as a Matching method and left other parameters as default values. We defined a landmark region containing the ROIs by clicking and dragging to draw a rectangle, and initiated the registration process. After image registration, ROIs (region of interest) corresponding to nerve bundle or cell bodies of labeled neurons were manually selected and the fluorescence intensity in the ROIs was measured using Fiji. The average fluorescence intensity during the first 15 s of image acquisition was used as the baseline to calculate the $\Delta F/F$. The mean of $\Delta F/F$ during the indicated periods was calculated and visualized using Python. For cell body analysis, we defined the positive response if the average $\Delta F/F$ during the photostimulation was statistically higher than the baseline ($p < 0.01$). The strong response neurons ($\Delta F/F > 0.4$) and the intermediate neurons ($0.15 < \Delta F/F \leq 0.4$) were defined based on the average $\Delta F/F$ value during the stimulation, respectively.

Author Contributions

Kiichi Watanabe, Conceptualization, Data curation, Formal analysis, Investigation, Methodology, Resource, Software, Visualization, Writing - original draft, Writing - review and editing; Hui Chiu, Resource; David J. Anderson, Conceptualization, Funding acquisition, Methodology, Project

administration, Supervision, Writing - original draft, Writing - review and editing.

Acknowledgements

We thank N.A. Pierce and M. Schwarzkopf for advice on HCR techniques; A. Sanchez for fly stock maintenance; S. Cao for advice on imaging experiments; B. Weissbourd for advice on catFISH experiments; G.M. Rubin, B.D. Pfeiffer, and S. Waddell for reagents; C. Chiu, G. Mancuso, and L. Chavarria for the laboratory management and administrative assistance; and members of the Anderson laboratory for valuable comments on this work. This work was supported by NIDA Grant R01 DA031389. D.J.A. is an Investigator of the Howard Hughes Medical Institute.

References

Anderson DJ (2016) **Circuit modules linking internal states and social behaviour in flies and mice** *Nat Rev Neurosci* **17**:692–704 https://doi.org/10.1038/nrn.2016.125

Arakawa S, Gocayne JD, McCombie WR, Urquhart DA, Hall LM, Fraser CM, Venter JC (1990) **Cloning, localization, and permanent expression of a Drosophila octopamine receptor** *Neuron* **4**:343–354 https://doi.org/10.1016/0896-6273(90)90047-J

Asahina K, Watanabe K, Duistermars BJ, Hoopfer E, González CR, Eyjólfsdóttir EA, Perona P, Anderson DJ (2014) **Tachykinin-Expressing Neurons Control Male-Specific Aggressive Arousal in Drosophila** *Cell* **156**:221–235 https://doi.org/10.1016/j.cell.2013.11.045

Bath DE, Stowers JR, Hörmann D, Poehlmann A, Dickson BJ, Straw AD (2014) **FlyMAD: Rapid thermogenetic control of neuronal activity in freely walking Drosophila** *Nat Methods* **11**:756–762 https://doi.org/10.1038/nmeth.2973

Brand a H, Perrimon N (1993) **Targeted gene expression as a means of altering cell fates and generating dominant phenotypes** *Development* **118**:401–15

Burke CJ, Huetteroth W, Owald D, Perisse E, Krashes MJ, Das G, Gohl D, Silies M, Certel S, Waddell S (2012) **Layered reward signalling through octopamine and dopamine in Drosophila** *Nature* **492**:433–7 https://doi.org/10.1038/nature11614

Buzsáki G (2004) **Large-scale recording of neuronal ensembles** *Nat Neurosci* **7**:446–451 https://doi.org/10.1038/nn1233

Cachero S, Ostrovsky AD, Yu JY, Dickson BJ, Jefferis GSXE (2010) **Sexual Dimorphism in the Fly Brain** *Current biology : CB* **20**:1589–1601 https://doi.org/10.1016/j.cub.2010.07.045

Chen S, Lee AY, Bowens NM, Huber R, Kravitz E a. (2002) **Fighting fruit flies: a model system for the study of aggression** *Proc Natl Acad Sci USA* **99**:5664–8 https://doi.org/10.1073/pnas.082102599

Chen X, Rahman R, Guo F, Rosbash M (2016) **Genome-wide identification of neuronal activity-regulated genes in drosophila** *eLife* **5**:1–21 https://doi.org/10.7554/eLife.19942

Chiu H, Hoopfer ED, Coughlan ML, Pavlou HJ, Goodwin SF, Anderson DJ (2021) **A circuit logic for sexually shared and dimorphic aggressive behaviors in Drosophila** *Cell* **184**:507–520 https://doi.org/10.1016/j.cell.2020.11.048

Choi HMT, Schwarzkopf M, Fornace ME, Acharya A, Artavanis G, Stegmaier J, Cunha A, Pierce NA (2018) **Third-generation in situ hybridization chain reaction: multiplexed, quantitative, sensitive, versatile, robust** *Development* **145**:dev165753–dev165753 https://doi.org/10.1242/dev.165753

Clowney EJ, Iguchi S, Bussell JJ, Scheer E, Ruta V (2015) **Multimodal Chemosensory Circuits Controlling Male Courtship in Drosophila** *Neuron* **87**:1036–1049 https://doi.org/10.1016/j.neuron.2015.07.025

Connolly JB, Roberts IJH, Armstrong JD, Kaiser K, Forte M, Tully T, O'Kane CJ (1996) **Associative Learning Disrupted by Impaired G s Signaling in Drosophila Mushroom Bodies** *Science* **274**:2104–2107 https://doi.org/10.1126/science.274.5295.2104

Dana H *et al.* (2019) **High-performance calcium sensors for imaging activity in neuronal populations and microcompartments** *Nat Methods* **16**:649–657 https://doi.org/10.1038/s41592-019-0435-6

Fernández MP, Kravitz EA (2014) **Aggression and Courtship in Drosophila: Pheromonal Communication and Sex Recognition** *J Comp Physiol A Neuroethol Sens Neural Behav Physiol* **119**:1065–76 https://doi.org/10.1007/s00359-013-0851-5

Flusberg BA, Nimmerjahn A, Cocker ED, Mukamel EA, Barretto RPJ, Ko TH, Burns LD, Jung JC, Schnitzer MJ (2008) **High-speed, miniaturized fluorescence microscopy in freely moving mice** *Nat Methods* **5**:935–938 https://doi.org/10.1038/nmeth.1256

Fujita N, Nagata Y, Nishiuchi T, Sato M, Iwami M, Kiya T (2013) **Visualization of neural activity in insect brains using a conserved immediate early gene, Hr38** *Current Biology* **23**:2063–2070 https://doi.org/10.1016/j.cub.2013.08.051

Greenberg ME, Greene LA, Ziff EB (1985) **Nerve growth factor and epidermal growth factor induce rapid transient changes in proto-oncogene transcription in PC12 cells** *J Biol Chem* **260**:14101–14110

Greenberg ME, Ziff EB (1984) **Stimulation of 3T3 cells induces transcription of the c-fos proto-oncogene** *Nature* **311**:433–438 https://doi.org/10.1038/311433a0

Grewe BF, Helmchen F (2009) **Optical probing of neuronal ensemble activity** *Current Opinion in Neurobiology* :520–529 https://doi.org/10.1016/j.conb.2009.09.003

Grover D, Katsuki T, Greenspan RJ (2016) **Flyception: Imaging brain activity in freely walking fruit flies** *Nat Methods* **13**:569–572 https://doi.org/10.1038/nmeth.3866

Grover D, Katsuki T, Li J, Dawkins TJ, Greenspan RJ (2020) **Imaging brain activity during complex social behaviors in Drosophila with Flyception2** *Nature Communications* **11** https://doi.org/10.1038/s41467-020-14487-7

Guzowski JF, McNaughton BL, Barnes CA, Worley PF (1999) **Environment-specific expression of the immediate-early gene Arc in hippocampal neuronal ensembles** *Nat Neurosci* **2**:1120–1124 https://doi.org/10.1038/16046

Hindmarsh Sten T, Li R, Otopalik A, Ruta V (2021) **Sexual arousal gates visual processing during Drosophila courtship** *Nature* **595**:549–553 https://doi.org/10.1038/s41586-021-03714-w

Hoopfer ED, Jung Y, Inagaki HK, Rubin GM, Anderson DJ (2015) **P1 interneurons promote a persistent internal state that enhances inter-male aggression in Drosophila** *eLife* **4**:1–27 https://doi.org/10.7554/eLife.11346

Inagaki HK, Jung Y, Hoopfer ED, Wong AM, Mishra N, Lin JY, Tsien RY, Anderson DJ (2014) **Optogenetic control of Drosophila using a red-shifted channelrhodopsin reveals experience-dependent influences on courtship** *Nat Methods* **11**:325–332 https://doi.org/10.1038/nmeth.2765

Jenett A *et al.* (2012) **A GAL4-driver line resource for Drosophila neurobiology** *Cell Rep* **2**:991–1001 https://doi.org/10.1016/j.celrep.2012.09.011

Jung Y, Kennedy A, Chiu H, Mohammad F, Claridge-Chang A, Anderson DJ (2020) **Neurons that Function within an Integrator to Promote a Persistent Behavioral State in Drosophila** *Neuron* **105**:322–333 https://doi.org/10.1016/j.neuron.2019.10.028

Karigo T, Kennedy A, Yang B, Liu M, Tai D, Wahle IA, Anderson DJ (2021) **Distinct hypothalamic control of same- and opposite-sex mounting behaviour in mice** *Nature* **589**:258–263 https://doi.org/10.1038/s41586-020-2995-0

Kim D-W *et al.* (2019) **Multimodal Analysis of Cell Types in a Hypothalamic Node Controlling Social Behavior** *Cell* **179**:713–728 https://doi.org/10.1016/j.cell.2019.09.020

Kim Y *et al.* (2015) **Mapping Social Behavior-Induced Brain Activation at Cellular Resolution in the Mouse** *Cell Reports* **10**:292–305 https://doi.org/10.1016/j.celrep.2014.12.014

Koganezawa M, Kimura K, Yamamoto D (2016) **The Neural Circuitry that Functions as a Switch for Courtship versus Aggression in Drosophila Males** *Current Biology* **26**:1395–1403 https://doi.org/10.1016/j.cub.2016.04.017

Lai S-L, Lee T (2006) **Genetic mosaic with dual binary transcriptional systems in Drosophila** *Nat Neurosci* **9**:703–9 https://doi.org/10.1038/nn1681

Lim RS, Eyjólfsdóttir E, Shin E, Perona P, Anderson DJ (2014) **How Food Controls Aggression in Drosophila** *PLoS ONE* **9** https://doi.org/10.1371/journal.pone.0105626

Lin D, Boyle MP, Dollar P, Lee H, Lein ES, Perona P, Anderson DJ (2011) **Functional identification of an aggression locus in the mouse hypothalamus** *Nature* **470**:221–226 https://doi.org/10.1038/nature09736

Morgan JI, Curran T (1991) **Stimulus-transcription coupling in the nervous system: involvement of the inducible proto-oncogenes fos and jun** *Annu Rev Neurosci* **14**:421–451 https://doi.org/10.1146/annurev.ne.14.030191.002225

Pfeiffer BD *et al.* (2008) **Tools for neuroanatomy and neurogenetics in Drosophila** *Proc Natl Acad Sci USA* **105**:9715–20 https://doi.org/10.1073/pnas.0803697105

Raap AK, van de Corput MPC, Vervenne RAM, van Gijlswijk RPM, Tanke HJ, Wiegant J. (1995) **Ultra-sensitive FISH using peroxidase-mediated deposition of biotin- or fluorochrome tyramides** *Hum Mol Genet* **4**:529–534 https://doi.org/10.1093/hmg/4.4.529

Remedios R, Kennedy A, Zelikowsky M, Grewe BF, Schnitzer MJ, Anderson DJ (2017) **Social behaviour shapes hypothalamic neural ensemble representations of conspecific sex** *Nature* **550**:388–392 https://doi.org/10.1038/nature23885

Renier N *et al.* (2016) **Mapping of Brain Activity by Automated Volume Analysis of Immediate Early Genes** *Cell* **165**:1789–1802 https://doi.org/10.1016/j.cell.2016.05.007

Saudou F, Amlaiky N, Plassat JL, Borrelli E, Hen R (1990) **Cloning and characterization of a Drosophila tyramine receptor** *The EMBO Journal* **9**:3611–3617 https://doi.org/10.1002/j.1460-2075.1990.tb07572.x

Schindelin J *et al.* (2012) **Fiji: an open-source platform for biological-image analysis** *Nat Methods* **9**:676–682 https://doi.org/10.1038/nmeth.2019

Schneider CA, Rasband WS, Eliceiri KW (2012) **NIH Image to ImageJ: 25 years of image analysis** *Nat Methods* **9**:671–675 https://doi.org/10.1038/nmeth.2089

Seelig JD, Chiappe ME, Lott GK, Dutta A, Osborne JE, Reiser MB, Jayaraman V (2010) **Two-photon calcium imaging from head-fixed Drosophila during optomotor walking behavior** *Nat Methods* **7**:535–540 https://doi.org/10.1038/nmeth.1468

Shao L, Chung P, Wong A, Siwanowicz I, Kent CF, Long X, Heberlein U (2019) **A Neural Circuit Encoding the Experience of Copulation in Female Drosophila** *Neuron* **102**:1025–1036 https://doi.org/10.1016/j.neuron.2019.04.009

Shen P, Wan X, Wu F, Shi K, Li J, Gao H, Zhao L, Zhou C (2023) **Neural circuit mechanisms linking courtship and reward in Drosophila males** *Current Biology* **33**:2034–2050 https://doi.org/10.1016/j.cub.2023.04.041

Sinigaglia C, Thiel D, Hejnol A, Houliston E, Leclère L (2018) **A safer, urea-based in situ hybridization method improves detection of gene expression in diverse animal species** *Developmental Biology* **434**:15–23 https://doi.org/10.1016/j.ydbio.2017.11.015

Stockinger P, Kvitsiani D, Rotkopf S, Tirián L, Dickson BJ (2005) **Neural circuitry that governs Drosophila male courtship behavior** *Cell* **121**:795–807 https://doi.org/10.1016/j.cell.2005.04.026

Takayanagi-Kiya S, Kiya T (2019) **Activity-dependent visualization and control of neural circuits for courtship behavior in the fly Drosophila melanogaster** *Proc Natl Acad Sci USA* **116**:5715–5720 https://doi.org/10.1073/pnas.1814628116

Takayanagi-Kiya S, Shioya N, Nishiuchi T, Iwami M, Kiya T (2023) **Cell assembly analysis of neural circuits for innate behavior in Drosophila melanogaster using an immediate early gene stripe / egr-1** *Proc Natl Acad Sci USA* **120** https://doi.org/10.1073/pnas.2303318120

Turner GC, Bazhenov M, Laurent G (2008) **Olfactory Representations by Drosophila Mushroom Body Neurons** *Journal of Neurophysiology* **99**:734–746 https://doi.org/10.1152/jn.01283.2007

von Philipsborn AC, Liu T, Yu JY, Masser C, Bidaye SS, Dickson BJ. (2011) **Neuronal Control of Drosophila Courtship Song** *Neuron* **69**:509–522 https://doi.org/10.1016/j.neuron.2011.01.011

Vosshall LB, Stocker RF (2007) **Molecular architecture of smell and taste in Drosophila** *Annual review of neuroscience* **30**:505–33 https://doi.org/10.1146/annurev.neuro.30.051606.094306

Wang L, Anderson DJ (2010) **Identification of an aggression-promoting pheromone and its receptor neurons in Drosophila** *Nature* **463**:227–31 https://doi.org/10.1038/nature08678

Wang L, Han X, Mehren J, Hiroi M, Billeter J-C, Miyamoto T, Amrein H, Levine JD, Anderson DJ (2011) **Hierarchical chemosensory regulation of male-male social interactions in Drosophila** *Nat Neurosci* **14** https://doi.org/10.1038/nn.2800

Watanabe K, Chiu H, Pfeiffer BD, Wong AM, Hoopfer ED, Rubin GM, Anderson DJ (2017) **A Circuit Node that Integrates Convergent Input from Neuromodulatory and Social Behavior-Promoting Neurons to Control Aggression in Drosophila** *Neuron* **95**:1112–1128 https://doi.org/10.1016/j.neuron.2017.08.017

Wilkie GS, Davis I (1998) **Visualizing mRNA by in situ hybridization using "high resolution" and sensitive tyramide signal amplification** *Technical Tips Online* **3**:94–97 https://doi.org/10.1016/S1366-2120(08)70110-7

Wilson RI, Turner GC, Laurent G (2004) **Transformation of Olfactory Representations in the Drosophila Antennal Lobe** *Science* **303**:366–370 https://doi.org/10.1126/science.1090782

Wu YE, Pan L, Zuo Y, Li X, Hong W (2017) **Detecting Activated Cell Populations Using Single-Cell RNA-Seq** *Neuron* **96**:313–329 https://doi.org/10.1016/j.neuron.2017.09.026

Yamamoto D, Koganezawa M (2013) **Genes and circuits of courtship behaviour in Drosophila males** *Nat Rev Neurosci* **14**:681–92 https://doi.org/10.1038/nrn3567

Yang B, Treweek JB, Kulkarni RP, Deverman BE, Chen C-K, Lubeck E, Shah S, Cai L, Gradinaru V (2014) **Single-Cell Phenotyping within Transparent Intact Tissue through Whole-Body Clearing** *Cell* **158**:945–958 https://doi.org/10.1016/j.cell.2014.07.017

Wan Yong, Otsuna H, Chien Chi-Bin, Hansen C (2009) **An interactive visualization tool for multi-channel confocal microscopy data in neurobiology research** *IEEE Trans Visual Comput Graphics* **15**:1489–1496 https://doi.org/10.1109/TVCG.2009.118

Yu JY, Kanai MI, Demir E, Jefferis GSXE, Dickson BJ (2010) **Cellular Organization of the Neural Circuit that Drives Drosophila Courtship Behavior** *Current biology : CB* **20**:1602–1614 https://doi.org/10.1016/j.cub.2010.08.025

Ziv Y, Burns LD, Cocker ED, Hamel EO, Ghosh KK, Kitch LJ, Gamal AE, Schnitzer MJ (2013) **Long-term dynamics of CA1 hippocampal place codes** *Nat Neurosci* **16**:264–266 https://doi.org/10.1038/nn.3329

Editors

Reviewing Editor
Esteban Beckwith
Universidad de Buenos Aires - CONICET, Buenos Aires, Argentina

Senior Editor
Albert Cardona
University of Cambridge, Cambridge, United Kingdom

Reviewer #1 (Public review):

Summary:

The authors have nicely demonstrated the efficiency of the HCR v.3.0 using hr38 mRNA expression as a marker of neuronal activity. This is very important in the Drosophila neuroscience field as in situ hybridization in adult Drosophila brains have been so far very challenging to do and replicate. The HCR v.3.0 has been described before [Choi et al., (2018)]

and is now the property of the non-profit organization Molecular Technologies, who are the ones responsible for designing the probes. Here, taking advantage of this new FISH method, the authors have demonstrated the use of the FISH to identify neurons activated by a specific behavioral task using hr38 mRNA as a marker of neuronal activation. They named their method HI-FISH.
In addition, based on the catFISH method [Guzowski et al., 1999], the authors were able to distinguish between newly activated neurons (nascent nuclear mRNA) and mature hr38 mRNA showing an earlier activation. They describe this method as HI-catFISH.
Finally, to test what are the neurons activated downstream of their neuronal group of interest, the authors combined the HI-FISH method with optogenetic using chrimson. They named this method opto-HI-FISH.

Using these three new methods, the authors have addressed the following biological question: are love and aggressiveness neuronally the same in Drosophila?
Here, the authors focused on the male specific P1a neurons which are activated by both an aggressive context (male-male encounter) and sexual context (male female encounter).

Strengths:

The demonstration of the efficiency of the method is very convincing and well-performed. It gives the will for the reader to apply the method to their own subject.

Weaknesses:

The more neurons are present, the more difficult it is to identify neurons. This is something to take into account when applying these methods.

https://doi.org/10.7554/eLife.92380.2.sa2

Reviewer #2 (Public review):

Summary:

Watanabe et al. introduce a novel approach for activity-dependent labeling of neural circuits in Drosophila at single-cell resolution, based on detecting the expression of the immediate early gene Hr38 using in situ hybridization. While activity mapping of neurons during specific behaviors is well-established in rodent models, its application in Drosophila has been limited, primarily due to technical constraints. By overcoming these challenges, this study tackles an important and timely issue, providing a foundational tool that will serve as a key reference in the field of circuit neuroscience.

Strengths:

The principal strength of this method lies in its versatility and high sensitivity. It can be applied to a broad range of biological questions and enables the investigation of dynamic transcriptional regulation across an unlimited number of genes with a strong signal-to-noise ratio. As such, it holds great potential for widespread use across research labs.

Weaknesses:

No major weaknesses; all concerns have been adequately addressed.

https://doi.org/10.7554/eLife.92380.2.sa1

Author response:

> ***Reviewer #1:***

Response to Public Review

We thank the reviewer for taking the time to carefully read our paper and to provide helpful comments and suggestions, most of which we have incorporated in our revised manuscript. One of this reviewer's (and reviewer #2's) main concerns was that the confocal images provided in some cases did not appear to reflect the quantitative data in the bar graphs. These images were provided only for illustrative purposes, to give the reader a sense of what the primary data look like. The reviewer may not have appreciated that the quantitative data reflect counts of RNA smFISH signals (dots) in hundreds of cells collected through z-stacks comprising multiple optical sections in multiple flies for each condition For example, in P1a control condition (in Figure 2A), we have analyzed 135 neurons from 8 individuals. There, the number of z-planes ranged from 3 to 8 per hemisphere. It is generally not possible to find a single confocal section that encompasses quantitatively the statistics that are presented in the graphs. Presenting the data as an MIP (Maximum Intensity Projection, i.e., collapsed z-stack) in a single panel would generate an image that is too cluttered to see any detail. We have now included, for the reader's benefit, additional example confocal sections in both a z-stack and from the opposite hemisphere, in Supplemental Figure S4D. We have also inserted clarifying statements in the text on p. 7 (lines 154-156).

Another suggestion from Reviewer #1 is that "it would be more informative to separate in the quantification between the GAL4-expressing neurons and the non-expressing ones" based on the presented pictures where more non-P1a neurons (that the reviewer speculates may be pC1-type neurons) are activated by a male-male encounter than by a male-female encounter, while the P1a-positive neurons seem to be more responsive during courtship behavior. In this paper, we were not looking at pC1 neurons and did not try to answer which neuronal population(s) outside of the P1a population is/are responsible for aggression and/or courtship. Rather, we focused on P1a neurons and addressed whether P1a neurons that induce both aggression and courtship behavior when they are artificially activated (Hoopfer et al. 2015) are also naturally activated during spontaneous performance of these two social behaviors. However, this result did not exclude the possibility that P1a neurons were inactive during naturalistic courtship or aggression. Our data in the current manuscript provide further experimental evidence in support of the idea that P1a neurons as a population play a role in both of these behaviors. Moreover, we provided data identifying P1a neurons activated only during aggression or during courtship (or both). However this does not exclude that pC1 or other neighboring populations are activated during aggression as well (See also the response to 'Recommendations For The Authors' and text lines 151-154).

In Figure 3, we used opto-HI-FISH to identify candidate downstream targets (direct or indirect) of P1a neurons. We used 50 Hz Chrimson stimulation to activate P1a neurons to induce expression of Hr38 and identified Kenyon cells in the mushroom body (MB) and PAM neurons (as well as pCd neurons) as potential downstream targets of P1a cells. In Figure 3 – supplement we performed calcium imaging of KCs and PAM neurons in response to P1a optogenetic stimulation to confirm independently our results from the Hr38 labeling experiments. That control was the purpose of that supplemental experiment.

Based on those imaging data, the reviewer asked the further question of which [natural] behavioral context induces Hr38 expression in these populations (i.e., mating or aggression). This question is reasonable because our calcium imaging data (Figure 3-supplement) showed that both Kenyon cells and PAM neurons are active only during photo-stimulation of P1a neurons. Our previous behavioral studies (Inagaki et al., 2014; Hoopfer et al., 2015) showed that 50 Hz photo-stimulation of P1a neurons in freely moving flies induced unilateral wing

extension during stimulation, while aggression was observed only after the offset of the stimulation (Hoopfer et.al., 2015). Based on the comparison of those behavioral data to the imaging results in this paper, the reviewer suggested that Kenyon cells and PAM neurons are activated during courtship rather than during aggression. This is certainly a possible interpretation. However it is difficult to extrapolate from behavioral experiments in freely moving animals to calcium imaging results in head-fixed flies, particularly with response to neural dynamics. Furthermore, Hr38 expression, like that of other IEGs (e.g., c-fos), may reflect persistently activated 2nd messenger pathways (e.g., cAMP, IP3) in Kenyon cells and PAM neurons that are not detected by calcium imaging, but that nevertheless play a role in mediating its behavioral effects. We still do not understand the mechanisms of how optogenetic stimulation of P1a neurons in freely behaving flies induces aggression vs. courtship behavior. Although 50 Hz stimulation of P1a neurons does not induce aggressive behavior during photo-stimulation, it is possible that this manipulation activates both aggression and courtship circuits, but that the courtship circuit might inhibit aggressive behavior at a site downstream of the MB (e.g., in the VNC). Once stimulation is terminated and courtship stops the fly would show aggressive behavior, due to release of that downstream inhibition (see Models in Anderson (2016) Fig 2d, e). In that case, there would be no apparent inconsistency between the imaging data and behavioral data. We agree that the reviewer's question is interesting and important but we feel that answering this question with decisive experiments is beyond the scope of this manuscript.

Finally, Reviewer #1 suggested a method to evaluate the Hr38 signals in the catFISH experiment of Figure 4. We appreciate their suggestions, but the way that we evaluated the Hr38 signals was basically the same as the way the reviewer suggested. We apologize for the confusion caused by the lack of detailed descriptions in the original manuscript. We have now revised the methods section to explain more clearly how we define the cells as positive based on Hr38EXN and Hr38INT signals.

Response to Recommendations for the authors:

> *"To strengthen the author's argumentation, I would distinguish in their quantification between gal4+ from the other [classes of neighboring neurons]" (Fig. 2 and 4)."*

Our focus in this paper was to ask simply whether P1a neurons are active or not active during natural occurrences of the social behaviors they can evoke when artificially activated. We did not claim that they are the only cells in the region that control the behaviors. It is not possible to compare their activation to that of 'other' cells neighboring P1a neurons without a separate marker to identify those cells driven by a different reporter system (e.g., LexA). This in turn would require repeating all of the experiments in Figs 2 and 4 from scratch with new genotypes permitting dual-labeling of the two populations by different XFPs, and quantifying the data using 4-color labeling. We respectfully submit that such curiosity-driven experiments, while in principle interesting, are beyond the scope of the present manuscript. However, we have inserted text to acknowledge the possibility that the aggression-activated Hr38 signals in P1a- cells neighboring P1a+ cells may correspond to other classes of P1 neurons (of which there are 70 in total) or to pC1 cells. Changes: Text lines 151-154.

> *"if the magenta dot is outside of the nuclei I would not count this as positive also the size of the dot seems to be a good marker of the reality of the signal). I would measure the intensity of the hr38EXN. A high Hr38EXN level associated with the presence of hr38INT would indicate that the cell has been activated during both encounters, while a lower hr38EXN with no hr38INT would suggest only an activation during the 1st behavioural context. Finally, a lower hr38EXN associated with the presence of hr38INT would suggest the opposite, an activation only during the 2nd behaviour."*

We agree that there are some tiny dot signals with hr38 INT probe that are more likely the background signals. We only counted the INT probe signals as positive when the cells had a clearly visible dot and also co-localize with the exonic probe's signal, as primary (un-spliced) Hr38 transcripts in the nucleus should be positive for both EXN and INT probes. Regarding the reviewer's latter comments, we agree with their interpretation of the catFISH results and that is how we interpreted them originally. We measured the intensity of hr38EXN expression and defined hr38EXN-labeled cells as "positive" when the relative intensity was 3σ >average, a stringent criterion. In the revised manuscript, we added more detailed information in the methods section regarding our criteria for defining cell types as positive.

> *"Knowing that the P1a neurons (using the split-gal4) can trigger only wing extension when activated by optogenetic 50Hz, I would test to which behavioral context the MB neurons and the PAM neurons positively respond to."*

As we answered in 'Response to Public Review,' our opto-HI-FISH experiments identified Kenyon cells in the mushroom body (MB) and PAM neurons (as well as pCd neurons) as potential downstream targets of P1a cells, using Hr38 labeling. The purpose of the calcium imaging experiment in Figure 3 – supplement was to confirm the P1a-dependent activation of KCs and PAM neurons using an independent method. In that respect this control experiment was successful in that methodological confirmation. The reviser raised an interesting question about how our calcium imaging experiments relate to our behavioral experiments, in terms of the dynamics of KC and PAM activation. A recent publication (Shen et al., 2023) revealed that courtship behavior has a positive valence and that activation of P1 neurons mimics a courtship-reward state via activation of PAM dopaminergic neurons. Therefore, it is reasonable to think that PAM neurons (and Kenyon cells as downstream of PAM neurons) are activated during female exposure. However those data do not exclude the possibility that inter-male aggression is also rewarding in Drosophila males, as it has shown to be in mice. This is an interesting curiosity-driven question that has yet to be resolved. Therefore, as mentioned in the 'Response to Public Review,' we feel that the additional experiment the reviewer suggests is beyond the scope of our manuscript.

Changes: None.

> *Minor comments:*
>
> *"Please provide different pictures from main fig2 and sup2 for the three common conditions (control, aggression, and courtship)."*

The data set for Figure 2 and Figure 2 supplement are from the same experiment. Because of the limited space, we just presented the selected key conditions ('Control', 'Aggression', and 'Courtship') in the main figure and put the complete data set (including these three key conditions) in the supplemental figure.

Changes: None

> *"Please, provide scale bars for the images."*
>
> *Also, Reviewer #2 commented, 'Scale bars are missing on all the images throughout the main and supplementary figures.'*

We have now added scale bars for each figure.

> *"Fig.1: "Is the chrimsonTdtom images from endogenous fluorescence? It is not said in the legend and anti-dsred is not provided in the material and method while anti-GFP is."*

We are sorry for the confusion and thank the reviewer for raising that question. The signals were native fluorescence, and we have now added that information to the figure legend.

> *P7: "As an initial proof-of-concept application of HI-FISH, we asked whether neuronal subsets initially identified in functional screens for aggression-promoting neurons (Asahina et al., 2014; Hoopfer et al., 2015; Watanabe et al., 2017) were actually active during natural aggressive behavior. These included P1a, Tachykinin-FruM+ (TkFruM), and aSP2 neurons". Please put the references to the corresponding group of neurons listed. For example: "These included P1a neurons [Hoopfer et al., 2015]".*

We have now added these references.

> *P9: "Optogenetic and thermogenetic stimulation experiments have shown that that P1a interneurons can promote both male-directed aggression and male- or female-directed courtship" typo*

We appreciate the reviewer for catching this error and have corrected the text.

> *(P10:" To validate this approach, we first asked whether we could detect Hr38 induction in pCd neurons, which were previously shown by calcium imaging to be (indirect) targets of P1a neurons". Reference [Jung et al., 2020]*

We have now added this reference.

> *Fig. 4A: Put the time scale on the diagram (3h adaptation-20min-30min rest-20min-10min rest-collect)*

We have now added the time scale in Figure 4A.

> ***Reviewer #2:***

Response to Public Review:

We thank the reviewer for their helpful comments and suggestions. We have addressed most of them in our revised manuscript. The main concern of Reviewer #2 was the temporal resolution of the HI-catFISH experiment shown in Figure 4 and Figure 4-Supplement. Our original manuscript illustrated temporal patterns of Hr38EXN and Hr38ITN signals concomitant with different behavioral paradigms (Figure 4B). The reviewer pointed out that the illustrated experimental design does not reflect the actual data shown in Figure 4-Supplement A-C. We believe this issue was raised because we drew the temporal pattern of Hr38EXN signals in Figure 4B based on the intensity of Hr38EXN signals (Figure 4-Supplement B) rather than based on the % number of positive cells (Figure 4-Supplement C). We have now revised the schematic time course of Hr38EXN signals in Figure 4B using the % of positive cells. We believe this change will be helpful for readers to understand better the experimental design since we used the % of positive cells to identify patterns of P1a neuron activation during male-male vs. male-female social interactions in Figure 4D. Another suggestion from Reviewer #2 was to add additional controls, such as the quantification of the intronic and exonic Hr38 probes after either only the first or second social context exposure. In response, we have now added the data from only the first social context (Figure 4C, and 4D, right column). These new data provides evidence that there are essentially no detectable Hr38INT signals 60 minutes later without a second behavioral context, while Hr38EXN signals are still present at the time of the analysis. Unfortunately, we are not able to provide the converse dataset with the second behavioral context only to show that Hr38 INT signals are detected. On this point, we call the reviewer's attention to Figure 4-supplement-S4A-C, which

show that the INT probe signals are detectable at 15 and 30 minutes following stimulation, but not at 60 minutes. In the experiment of Fig. 4B, flies are fixed and labeled for Hr38 30 minutes after the beginning of the second behavior, conditions under which we should obtain robust INT signals (as observed). EXN signals are also expected at 30 minutes because the primary (non-spliced) RNA transcript detected by the INT probe also contains exonic sequences.

Response to Recommendations for the authors:

> *Given that the development of in situ HCR for the adult fly brain is so central to the present manuscript, I think that the methods section describing the HCR protocol can be significantly improved. In particular, the authors should fully describe the in situ HCR protocol including the 'minor modifications' they refer to, and define how they calculate the 'relative intensity to the background'.*

We appreciate the reviewer's suggestion. We have now revised the methods section to describe the procedure in more detail. Also, we will submit a separate document describing the HI-FISH protocol.

> *Note: The authors refer to a recently published paper by Takayanagi-Kiya et al (2023) describing activity-based neuronal labeling using a different immediate early gene, stripe/egr-1. The authors state the following: 'That study used a GAL4 driver for the stripe/egr-1 gene to label and functionally manipulate activated neurons. In contrast, our approach is based purely on detecting expression of the IEG mRNA using..'. Takayanagi-Kiya et al. (2023) also use in situ mRNA detection of the IEG stripe/egr-1 and not only a GAL4 driver system. This claim should be modified and the paper should be cited in the introduction of the present paper.*

We have now cited the paper in the Introduction and have modified and moved the description originally in 'Note' section to Discussion (text lines: 392-404) as the reviewer requested. We have emphasized the difference between the two approaches for comparing neuronal activities during two different behaviors within the same animal. Takayanagi-Kiya used GAL4/UAS and stripe protein expression with immunohistochemistry to analyze neuronal activities during two different behaviors, while we exclusively analyzed Hr38 mRNA expression for this purpose, using intronic and exonic Hr38 probes. This approach made it possible to perform catFISH with higher temporal resolution and also allows extension of our approach to other IEGs for which antibodies are not available.

> *Please specify the nature of the iron fillings in the methods section.*

We added a detailed description in the methods section, including the catalog number.

> *In Figure 1B, the authors may add a dashed outline to the regions magnified in 1C so that readers can more easily follow the figures. Moreover, it would be informative to see a more detailed quantification of the number of Hr38-positive cells in different brain regions marked by Fru-GAL4.*

We have now added the whole brain images for each condition in Figure 1C and also quantitative data in Figure 1-Supplement C, as the reviewer suggested.

> *In the middle right aggression panel of Figure 2A, it looks as if one P1a neuron is not outlined.*

We have carefully examined other z-planes through this region and based on those data have concluded that the signals mentioned by the reviewer are neurites from neurons labeled in other z-planes.

Changes: None.

> *The images in Figure 2A can be again found in Figure Supplement 2A, yet the number of neurons analyzed suggests the quantification was performed from different samples. The images in Figure Supplement 2A should be either changed or it should be explained as to why the images are the same yet the numbers in the legend are different.*

We apologize for the confusion. Figure 2 and Figure 2-Supplement are from the same experiment. To avoid clutter we illustrated three key conditions ('Control,' 'Aggression,' and 'Courtship') in the main figure. The reason why the numbers in the legend are different is that the purpose of presenting Figure 2-Supplement B-D was to determine whether there were differences in the intensity of Hr38 FISH signals in the neurons considered as 'positive' in different conditions. Therefore, the numbers described in Figure 2-Supplement legend are derived only from those neurons that were considered Hr38-positive, while the numbers in Figure 2 include all neurons analyzed. We have now added notes to explain this in the Figure 2 – supplement legend.

> *The panels of the quantification of the Hr38 relative intensity in Figure 2B/C/D are very difficult to read, ideally, they should be plotted as in Figure Supplement 2B/C/D.*

The graphs in Figure 2B-D (upper) show data from all GFP-labeled cells scored, including cells defined as 'negative' or 'borderline.' In contrast, the graphs in Figure 2-supplement show the relative Hr38 signal intensity in those GFP neurons defined as positive based on the analysis in Fig. 2B. If we were to plot the data in Fig. 2B (upper) as box plots (like that in Figure-2-supplement), we would see either a skewed (only negative cells) or a bimodal distribution (one around the negative population and the other around the positive population); the shapes of these distributions would likely be hidden in the box-whisker plots format. Therefore, we prefer to plot all of the data points as we did in the original manuscript. However, we agree that the data points in the original manuscript were hard to read. We therefore changed the format of the datapoints from blurry dots to open circles with clear solid lines.

> *In Figure 2B/C/D, please specify in the figure legend what 'grouped in categories according to character' means.*

We used letters to mark statistically significant differences (or lack thereof) between conditions. Bars sharing at least one common letter are not significantly different. If they do not share any letter, they are significantly different. For example, Aggression: bc vs. Dead: bc, means no difference. Aggression: bc vs. No Food: b, or Aggression: bc vs. Courtship: c also means no difference between Aggression and each of the two other conditions. However, 'No Food: b' and 'Courtship: c' have no common letter, meaning they are different. This is a standard method for showing statistically comparisons among multiple bars without lots of asterisks and horizontal bars cluttering the figure, and we have revised the legend to clarify what each letter means. We have also removed the color shading in Figure 2 B-D as it may have been confusing.

> *A quantification of the number of Hr38-positive neurons and Hr38 relative intensity during the entire time course would be informative in Figure 3D.*

Although the data set for this figure is different from that for Figure 4-Supplement A-C, the main claim is the same. Therefore, Figure 4 - Supplement essentially provides the information that the reviewer suggested. However, we also reanalyzed the data set used for the original Figure 3D and evaluated % positive cells at the 30-minute time point and have now added that number in the figure legend.

> *In the legend of Figure 3D, it says '..The expression level reaches its peak at 30-60min', yet I don't see timepoints beyond 60min. Please rephrase or add additional timepoints.*

We apologize for the error. We have rephrased the text.

> *Figure Supplement 3A/D: please add an outline or a schematic figure to better understand where the imaging is performed.*

We added illustrated schemas next to the title of each experiment (P1->PAM neurons (bundle) and P1 -> Kenyon cells (bundle)).

> *Figure Supplement 3C/F: please add information about the statistical test to the corresponding figure legend.*

We have added a phrase to describe the test used.

> *Figure Supplement 3G/H/I/J: motion artifacts can potentially strongly affect the performed analysis given that cell bodies are very small and highly subjected to motion. Can the authors comment on how they corrected for motion?*

We have now described how we corrected for motion artifacts in the Methods section.

> *Figure 4C/D: It seems as if the representative images don't reflect the quantification, e.g., in the male -> female panel, close to 100% of the neurons are positive for the exonic probe as opposed to approx. 40% in the bar graph.*

Please see our response to this issue in the 'Response to Public Review (Reviewer #1)'.

> *Additional controls should be included in Figure 4C in order to assess the temporal resolution of HI-CatFISH more in detail (see 'Weaknesses').*

We have also answered this in the 'Response to Public Review'.

> *The authors should adjust the scheme in the main Figure 4B to reflect the data presented in Figure S4A and C. For instance, the peak for the intronic version is observed at 15 minutes, while at 30 minutes, both the exonic and intronic signals show an equal level of signal.*

We have addressed this issue in the 'Response to Public Review'.

We thank the reviewers again for their helpful comments and hope that with these changes, the manuscript will now be acceptable for official publication in eLife.

https://doi.org/10.7554/eLife.92380.2.sa0